JMEPEG (2011) 20:894–902
DOI: 10.1007/s11665-010-9713-2

1059-9495/$19.00

Modeling and FE Simulation of Quenchable High Strength Steels Sheet Metal Hot Forming Process

Hongsheng Liu, Jun Bao, Zhongwen Xing, Dejin Zhang, Baoyu Song, and Chengxi Lei

(Submitted August 11, 2009; in revised form July 11, 2010)

High strength steel (HSS) sheet metal hot forming process is investigated by means of numerical simulations. With regard to a reliable numerical process design, the knowledge of the thermal and thermo-mechanical properties is essential. In this article, tensile tests are performed to examine the flow stress of the material HSS 22MnB5 at different strains, strain rates, and temperatures. Constitutive model based on phenomenological approach is developed to describe the thermo-mechanical properties of the material 22MnB5 by fitting the experimental data. A 2D coupled thermo-mechanical finite element (FE) model is developed to simulate the HSS sheet metal hot forming process for U-channel part. The ABAQUS/explicit model is used conduct the hot forming stage simulations, and ABAQUS/implicit model is used for accurately predicting the springback which happens at the end of hot forming stage. Material modeling and FE numerical simulations are carried out to investigate the effect of the processing parameters on the hot forming process. The processing parameters have significant influence on the microstructure of U-channel part. The springback after hot forming stage is the main factor impairing the shape precision of hot-formed part. The mechanism of springback is advanced and verified through numerical simulations and tensile loading-unloading tests. Creep strain is found in the tensile loading-unloading test under isothermal condition and has a distinct effect on springback. According to the numerical and experimental results, it can be concluded that springback is mainly caused by different cooling rats and the nonhomogengeous shrink of material during hot forming process, the creep strain is the main factor influencing the amount of the springback.

Keywords finite element, high strength steel, hot forming, numerical simulation, springback

1. Introduction

The increasing demand for better fuel economy, higher operating efficiency, and for the respective reduction of CO, CO_2, and NO_x emissions in automotive engines as wells as industrial and in aviation gas turbines has prompted intensive search for weight-saving structural materials. Although the application of aluminium sheets to automobile parts is attractive for the reduction in weight (Ref 1), high cost and low formability are crucial problems associated with the material, and thus the industry still has a great interest in steel sheets. The steel sheet with a tensile strength greater than 800 MPa has been developed recently. Since the international co-operative ultra-light steel auto body project has been advanced, the use of HSS sheets for automobile body panels has rapidly increased. However, the application of HSS sheet is yet limited because the springback is a main factor seriously impairing the shape precision of part which is cold formed by HSS sheet. The amount of springback after HSS sheet cold forming is in direct proportion to tensile strength because in the HSS sheet forming process elastic deformation has an increasing proportion of total deformation. Formability of HSS sheet gets lower as the tensile strength of HSS increases (Ref 2). Researchers focused on cold forming of HSS sheet to study the influence of forming processing parameters on quality of forming (Ref 3, 4). However, for cold forming process of the HSS sheet metal, the large amount of springback and low formability are the crucial problems, and limit the application of HSS sheet in automotive industry. In order to further expand the application of HSS sheet in automotive industry, the die quenching process (Ref 5, 6) also called hot stamping method was proposed to perform the HSS sheet metal forming at elevated temperature. Within the innovative hot stamping which is a non-isothermal forming process, it is possible to combine forming and quenching in one process step. The component finally exhibits a microstructure martensite with strength more than 1500 MPa through the hot forming technology. Prior to hot forming process, the blank must be austenitized for 5-10 min in furnace at 900-950 °C. On achieving a homogeneous microstructure austenitic, the blank is transferred to the water cooled die, where forming and quenching take place simultaneously. Hot stamping affords the opportunity to manufacture components with complex geometric shapes, high tensile strength, and a minimum of springback, which currently find applications as crash relevant components in the automotive industry. Hot forming method is an effective way to improve formability of HSS sheet metal and reduce deformation resistance as well as the amount of springback (Ref 7). Springback after HSS sheet metal hot forming was predicted through numerical simulations and visco-plastic crystal plasticity models (Ref 8).

Hongsheng Liu, Jun Bao, Zhongwen Xing, Dejin Zhang, Baoyu Song, and **Chengxi Lei**, Department of Mechatronics Engineering, Harbin Institute of Technology, P.O. Box 425, Harbin 150001, People's Republic of China. Contact e-mail: hs_liu_hit@163.com.

The influence of forming temperature on springback was examined, and the forming temperature was optimized in Ref 9. In order to examine thermo-mechanical flow properties of HSS sheet metal in the hot forming process, the model for describing the relationship between flow stress and temperature, strain as well as strain rate were established through experiments (Ref 10). Since HSS sheet metal hot forming is a complex forming process related with material nonlinearity, heat effect, geometric nonlinearity and complex thermo-mechanical properties etc., it is difficult to solve the problem encountered in the practical production by means of analytical and experimental methods (Ref 11). In this article, numerical method is employed to investigate the HSS sheet metal hot forming process. The thermal and thermo-mechanical properties are determined and examined through hot tensile tests using a modified Gleeble 1500 system, and material model for evaluating the material flow stress at different strains, strain rates, and temperatures is developed. Numerical simulations of HSS sheet metal hot forming for U-channel part are carried out to investigate the influence of processing parameters on the hot forming process. To develop the mechanism of springback, the main causes of springback are analyzed through numerical simulations and experiments.

2. Modeling

The accurate numerical simulations of HSS sheet metal hot forming is strongly related with the proper description of the material flow stress at different strains, strain rates, and temperatures. To determine the material flow stress at elevated temperature, tensile tests are carried out through a modified Gleeble 1500 system. Considering the resulting microstructure in terms of grain size show in Fig. 1, an austenitization temperature equal to 950 °C together with a holding time of 3 min assures a complete austenitization. Therefore, before the tensile tests, the specimens should be heated to an austenitization temperature of 950 °C. After leaving the specimen at 950 °C for about 3 min, rapid cooling and stabilization at target temperatures, for example, 500, 660, and 860 °C for about 5 s take place. Afterward, the tensile test was carried out under isothermal conditions. The influence of deformation temperature on the flow properties of the test material 22MnB5 has been investigated at different strains and strain rates and temperatures in the austenitic state after rapid cooling. Figure 2 shows the relationship between the true stress and the true strain for temperatures like 500, 660 and 860 °C and strain rate of 1.0 s^{-1}. It can be seen from Fig. 2 that the temperature has a significant influence on the flow properties of the material, and increasing temperature leads to a apparent decrease of flow stress and the slop of stress-strain curve. For the lower strain rate such as $d\varepsilon/dt = 0.1\ s^{-1}$, the material shows the same dependency of temperature as shown in Fig. 3. In addition, the recovery process occurs during hot deformation at the temperature above 660 °C, and therefore, the recovery leads to the plane flow stress-strain curve. The influence of temperature on flow stress is more apparent: the higher the temperature is the lower the strain rate is. According to the experimental results shown in Fig. 2 and 3, respectively, the strain rate seems to have the same influence on the flow stress of the test material. Therefore, the influence of strain rate on the flow stress has to

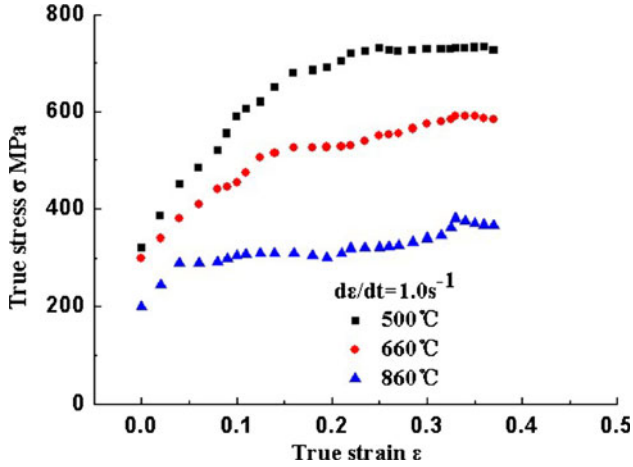

Fig. 2 Influence of deformation temperature on the flow properties of 22MnB5 HSS for strain rate of 1.0 s^{-1}

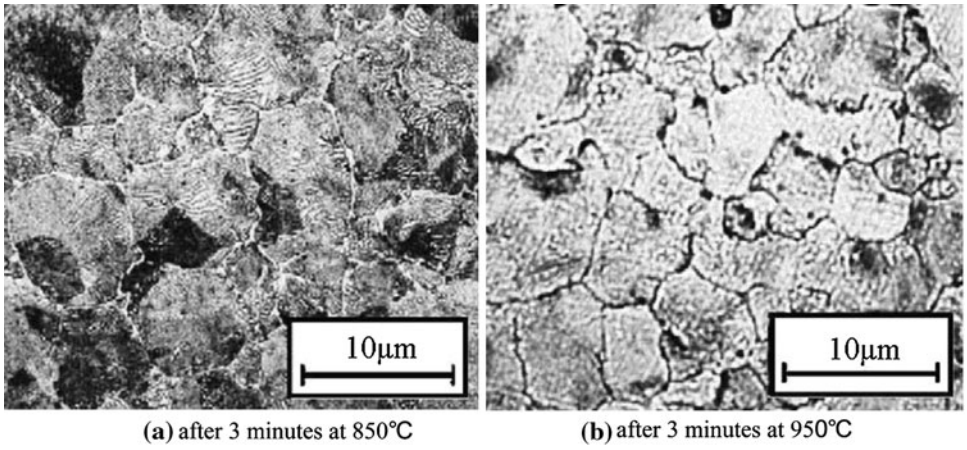

Fig. 1 Micrographs of austenitized specimens: (a) after 3 min at 850 °C and (b) after 3 min at 950 °C

be considered for different strain rates regarding the characterization of the material characteristics at elevated temperatures. The dependency of the material flow behavior on the strain rate has been investigated for three different strain rates of 0.01, 0.1, and 1.0 s^{-1} after rapid cooling to 600 °C. According to the results shown in Fig. 4, it is obvious that the strain rate has a significant effect on the material deformation behavior. Increasing the strain rate leads to an apparent increase of the flow stress, and the slope of stress-strain curve as a consequence of an enforced work hardening of the material.

The phenomenological approach according to Eq 1 is used for modeling the flow behavior of the material 22MnB5 in respect of dependency of strain, strain rate, and temperature. The commercial software ORINGIN is used to fit the stress-strain relationship by applying the constitutive relation:

$$\sigma(\varepsilon, \dot{\varepsilon}, T) = K \cdot \exp(\beta/T) \cdot (\varepsilon_0 + \varepsilon)^{n_0 \cdot \exp(-c_n(T_i - T_0))} \cdot \dot{\varepsilon}^{m_0 \cdot \exp(c_m(T_i - T_0))} \quad \text{(Eq 1)}$$

where K = 33.56, n_0 = 0.2236, c_n = 0.0021, ε_0 = 0.0025, β = 2341.78, m_0 = 0.0756, and c_m = 0.0022.

The strain-stress curves fitted by Eq 1 are compared in Fig. 5-7 with experimental data for various strain rates and temperatures. In the development of constitutive model, the work hardening behaviors of a material at different strains,

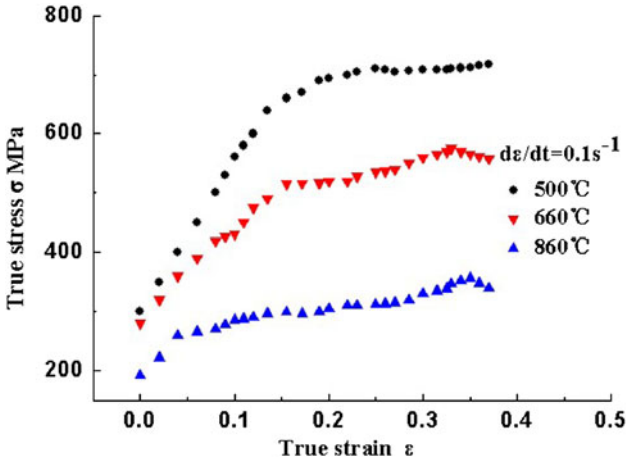

Fig. 3 Influence of deformation temperature on the flow properties of 22MnB5 HSS for the strain rate of 0.1 s^{-1}

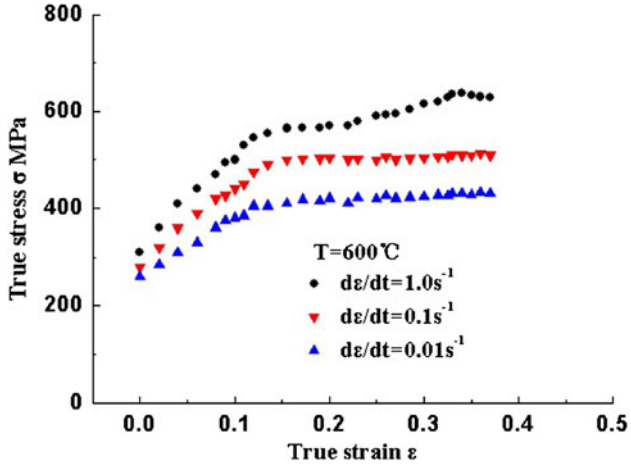

Fig. 4 Influence of strain rate on the flow properties of 22MnB5 HSS for deformation temperature of 600 °C

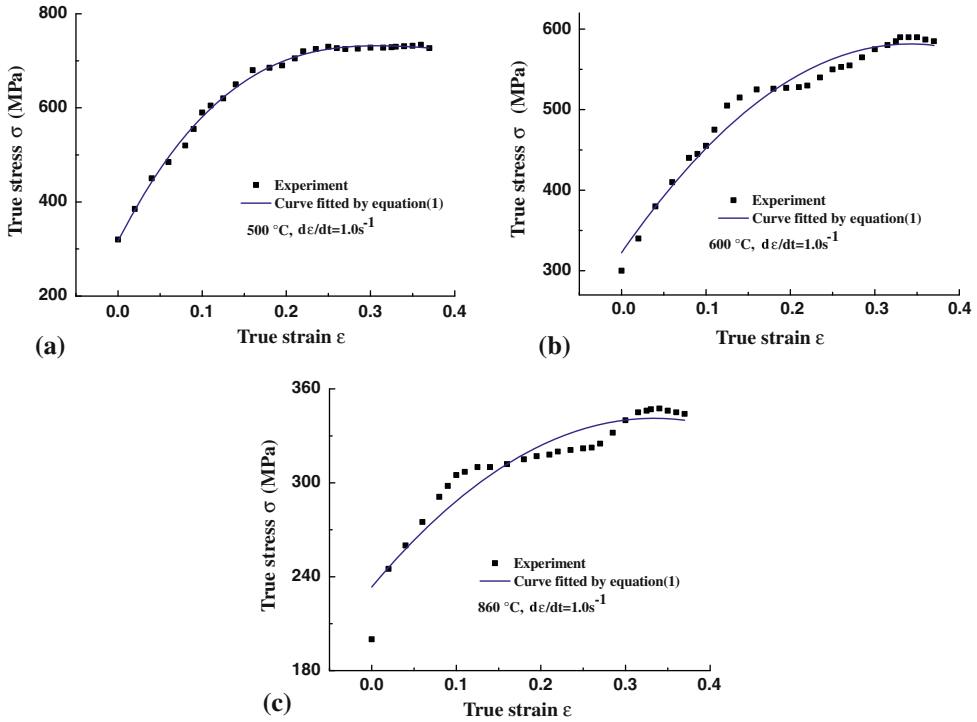

Fig. 5 Stress-strain relationship between experimental data and constitutive model for different temperatures, and at the strain rate of 1.0 s^{-1}

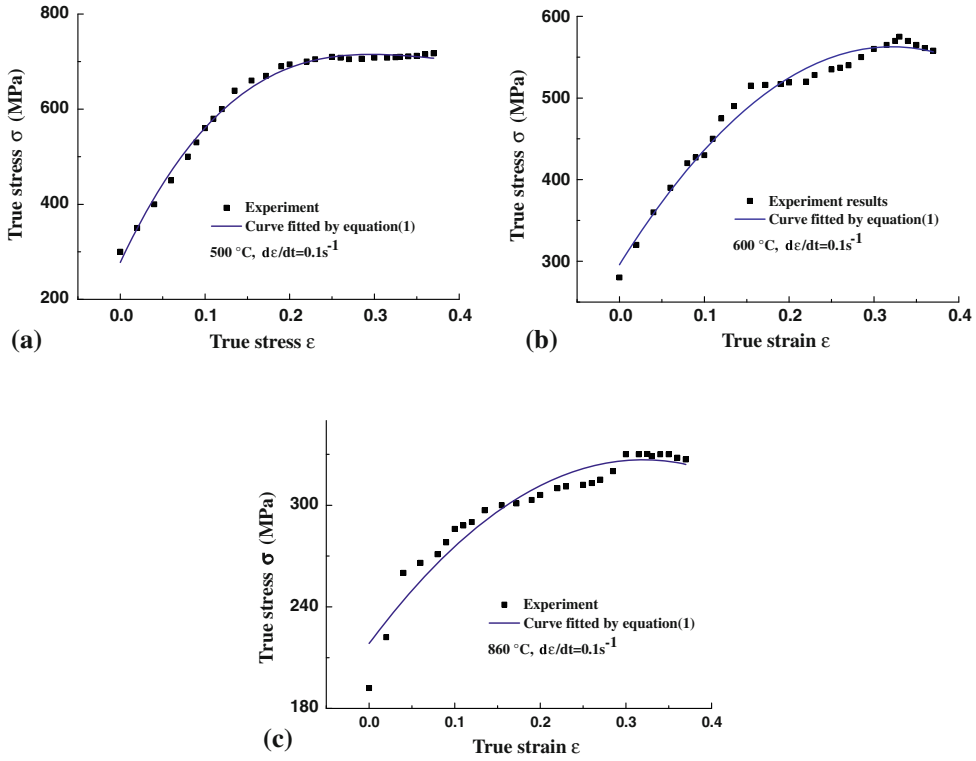

Fig. 6 Stress-strain relationship between experimental data and constitutive model for different temperatures, and at the strain rate of 0.1 s^{-1}

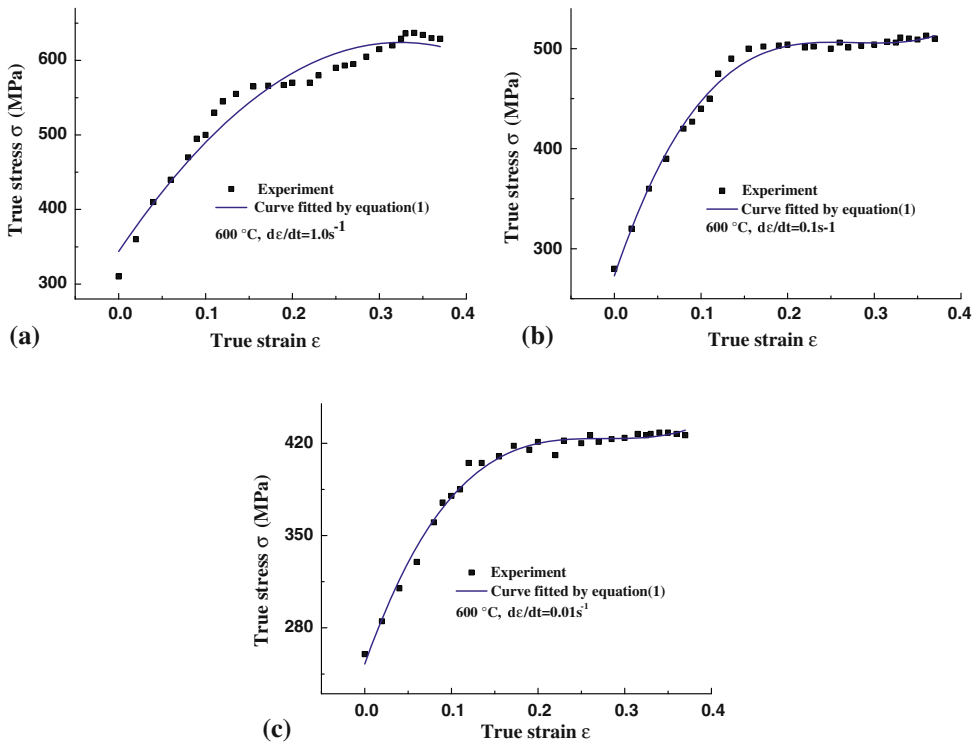

Fig. 7 Stress-strain relationship between experimental data and constitutive model for different strain rates, and at the temperature of 600 °C

strain rates, and temperatures are described in Fig. 5-7. Figures 5-7 show that the constitutive model can follow the work hardening behavior of the material up to saturation stress under any combination of temperature and strain rate. Moreover, it can be observed that the work hardening rate becomes lower as the temperature increases. The work

hardening rate $\theta = \partial\sigma/\partial\varepsilon$ represents the slope of the stress-strain curve.

3. FE Model for Non-Isothermal Hot Forming Process for U-Channel Part

In order to investigate the hot forming process, the numerical simulations of hot forming process for U-channel part are carried out. As shown in Fig. 8, the hot forming process consists of four stages: (a) exerting blank holder force (BHF) on the holder, (b) hot forming, (c) quenching, in this stage punch, die, and holder keep remaining in contact with the workpiece for seconds, the U-channel part gets rapidly cooled and fully quenched, and (d) removal of punch and holder: in this stage, springback takes place. Therefore, the hot forming is a non-isothermal forming process. The ABAQUS/explicit model is used to conduct the hot forming stage simulations, and ABAQUS/implicit model is used to accurately predict the springback which happens after hot forming stage.

Timeslices used in each corresponding analysis step are the following: 0-0.0001 s used in analysis of exerting BHF, 0.0001-0.9001 s used in analysis of hot forming, 0.9001-6.9001 s used in analysis of quenching, and 6.9001-10.7001 s used in analysis of springback. FE models of die, punch, holder, and blank used in the hot forming simulations for U-channel part, are shown in Fig. 8. The size of die cavity d_D is varied to examine the influence of die gap on the hot forming process. The size of blank is 430 mm × 230 mm × 2 mm. In the FE models, blank is defined as deformable body and the tools such as punch, die, and holder are defined as rigid bodies. The types of meshes, the number of meshes, and the quality of mesh are considered in the FE models. The blank, punch, die, and holder are discretized through meshes of CPE4RT in the forming stage simulations, the meshes of CPE4RT are used to discretize the formed part in springback simulations. In order to accurately predict the springback, the blank is discretized by three lays of meshes shown in Fig. 8. Compared to the sheet metal cold forming, besides the geometrical contact, the thermo-contact must be considered in the hot forming. As shown in Fig. 8, there are five geometrical contact surfaces, namely, die geometrical contact surface (DGCS), punch geometrical contact surface (PGCS), holder geometrical contact surface (HGCS), upper blank geometrical contact surface (UBGCS), and lower blank geometrical contact surface (LBGCS). The five contact surfaces are used to analyze the heat transference from blank to tools and to treat geometrical contact between blank and tools. Traditional penalty method is used to treat the geometrical contact.

In order to treat thermo-contact, besides the above five contact surfaces, other four surfaces remaining in contact with air should be defined, namely, die thermo-contact surface (DTCS), punch thermo-contact surface (PTCS), holder thermo-contact surface (HTCS), and blank thermo-contact surface (BTCS), as shown in Fig. 8. The four contact surfaces are used to analyze heat exchange between blank and tools as well as air. Corresponding to different contact surfaces, the ways of heat transference are different. There are nine contact pairs, as shown in Fig. 8, which are used for treating the thermo-contact.

The blank loses heat by convection and radiation heat transfer to the environment when the blank is transferred from the oven to the tools. When the hot blank contacts the tools, the hot blank begins to lose heat by thermo-contact conductance. Therefore, the determinations of convection coefficients, radiation coefficients, and thermo-contact conductance dependent on the contact pressure are crucial to accurately compute the variation of temperature on the blank in the hot forming. These coefficients can be determined by means of hot forming tests. B. Shapiro (Ref 12) obtained the convection coefficients, and radiation coefficients shown in Table 1 through empirical formulas, Merklein (Ref 13) presented the thermo-contact conductance shown in Table 1. In this article, the coefficients

Table 1 Convection, radiation, and thermo-contact conductance coefficients (Ref 12, 13)

T, °C	h_{conv}, W/m^2 °C	h_{rad}, W/m^2 °C	P, MPa	h_{cond}, W/m^2 °C at 550 °C
50	5.68	5.31	0	750
100	6.80	6.80	5	1330
200	7.80	10.80	10	1750
300	8.23	16.3	20	2500
400	8.43	23.6	35	…
500	8.51	33.0	40	3830
600	8.52	44.8		
700	8.50	59.3		
800	8.46	76.6		
900	8.39	97.2		
1000	8.32	141		

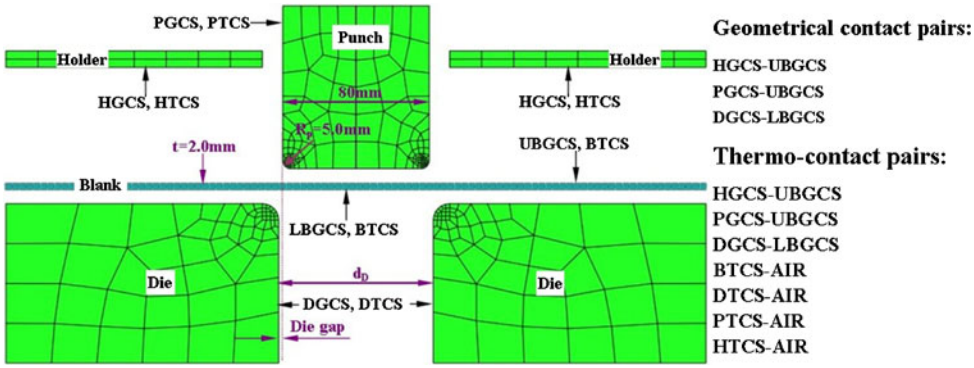

Fig. 8 2D coupled thermo-mechanical FE model for U-channel part forming

shown in Table 1 are used for computing the heat transference in hot forming.

4. Numerical Results and Discussion

Aiming at confirming the effect of processing parameters on the hot forming process, the numerical simulations of non-isothermal forming processes for U-channel part under different processing parameters are conducted under the ABAQUS environment. The springback seriously impairs the quality of the hot-formed part. Two measurements, namely, the springback of wall opening angle θ_{sb} and the springback of flange angle θ_{sf} are shown in Fig. 9. The amount of flange springback is defined as $\Delta\theta_f = \theta_{sf} - 90^\circ$ and the amount of sidewall springback is defined as $\Delta\theta_s = \theta_{sb} - 90^\circ$.

4.1 Influence of BHF on Hot Forming

The influence of BHF on springback is investigated through HSS sheet metal hot forming process simulations with die profile radius of 10.0 mm and die gap of 2.6 mm. Figure 10 shows the distribution of temperature on U-channel part for different BHFs at the end of quenching stage. It can be seen from Fig. 10 that the BHF has a significant influence on the distribution of temperature on the flange of U-channel part and that the minimum of temperature of the flange decreases with BHF increasing because of that the thermo-contact conductance varies directly with the contact pressure, which is directly related to BHF. It means that more heat will be lost from the flange with the increasing BHF. Another reason is that the BHF has an important influence on the contact state between the blank and the die. The end of flange is in good contact with the die while their BHFs aree 1.0 and 3.5 MPa, respectively. On the other hand, the middle of the flange has good contact with die while the BHF is 2.5 MPa.

It can been seen from Fig. 10 that the microstructure of flange is the combination of most of martensite and few of upper bainite with BHF of 1.0 MPa. The cooling rate of flange becomes higher as BHF increases, the microstructure austenite is transformed into martensite completely with BHF of 3.5 MPa. The influence of BHF on springback is investigated, and Fig. 11 shows that increasing the BHF leads to an apparent reduction in springback. The deformation model at flange angle and sidewall angle is bending deformation, with BHF increasing the more amount of friction is exerted on the flange, therefore, tensile stress zone within bending deformation zone is enlarged, as a consequence, springback is reduced drastically while the BHF is increasing.

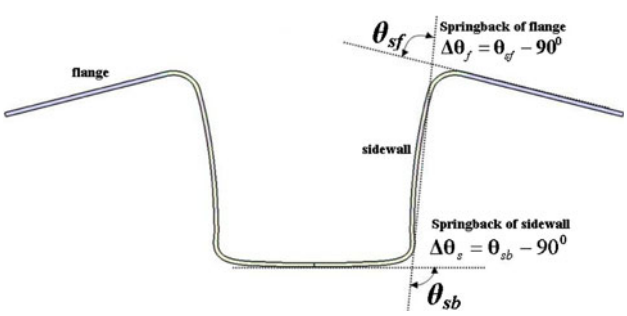

Fig. 9 Definition of springback

4.2 Influence of Die Gap on Hot Forming

The sidewall of U-channel part cannot be fully quenched due to die gap in the hot forming, the microstructure austenitic in the sidewall of U-channel cannot be transformed into martensite richly to improve the tensile strength of part. Figure 12 shows the distribution of temperature on sidewall for different BHFs at the end of quenching. The die gap has a significant influence on the distribution of temperature on the sidewall. The microstructure of sidewall with different die gaps shown in Fig. 12 reveals that the microstructure mainly comprises martensite while die gap is 3.0 mm, the main cause is that the sidewall cannot be fully quenched, as consequence of that, the microstructure austenitic is not transformed into martensite completely. With the die gap becoming smaller, the sidewall can be cooled at higher cooling rate and thus fully quenched. The microstructure in the sidewall can be transformed into martensite completely with the die gap of 2.05 mm as shown in Fig. 12(a). The influence of die gaps on the springback is examined through numerical simulations shown in Fig. 13. As shown in Fig. 13, increasing die gap leads to an apparent increase in springback, and, with the die gap more than 2.5 mm, the flange springback is larger than sidewall springback with the same die gap. Besides, it can be seen from Fig. 13 that the simulation results have a good consistency with the experimental results.

The influence is caused by die gap and heat effect originating from non-uniform cooling, as explained through Fig. 14. It can be seen from Fig. 14 that the flange angle θ_{sf} and sidewall angle θ_{sb} becomes more and more large as the die gap

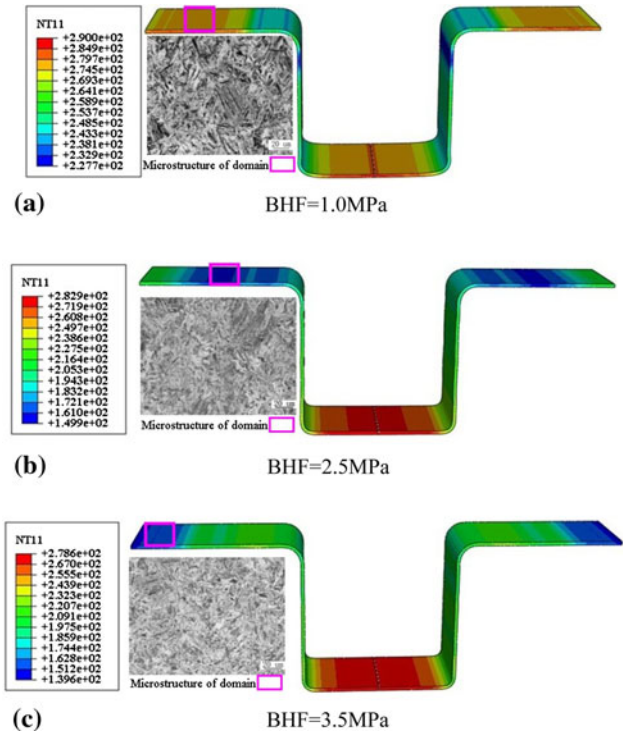

Fig. 10 Influence of BHF on the distribution of temperature on U-channel part

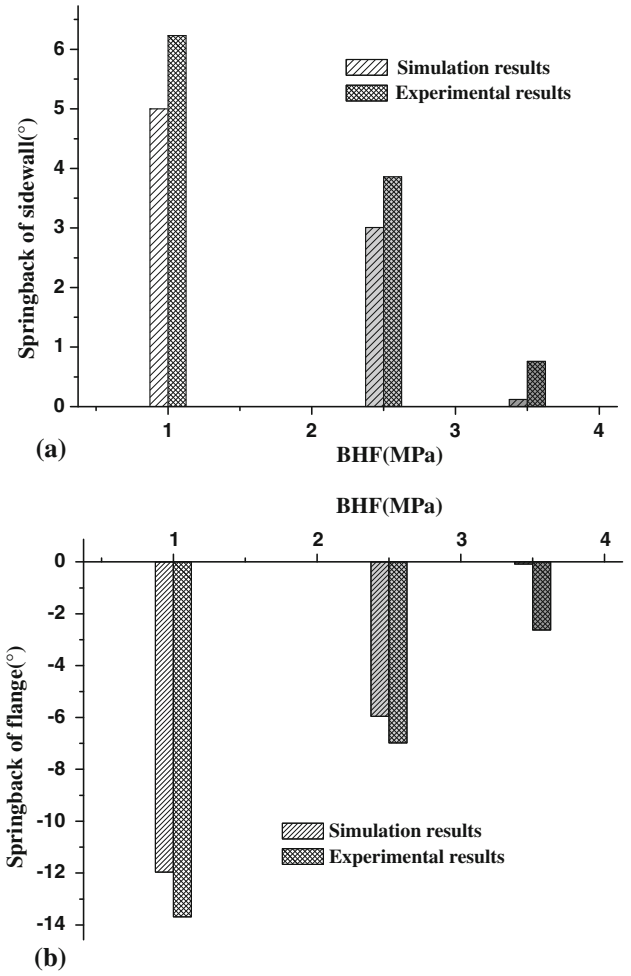

Fig. 11 Influence of BHF on spring-back

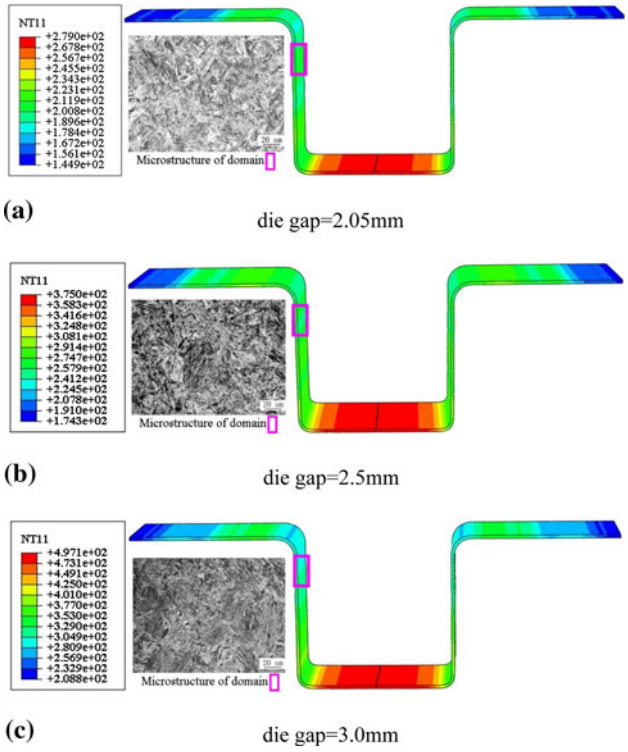

Fig. 12 Influence of die gap on distribution of temperature on the side wall

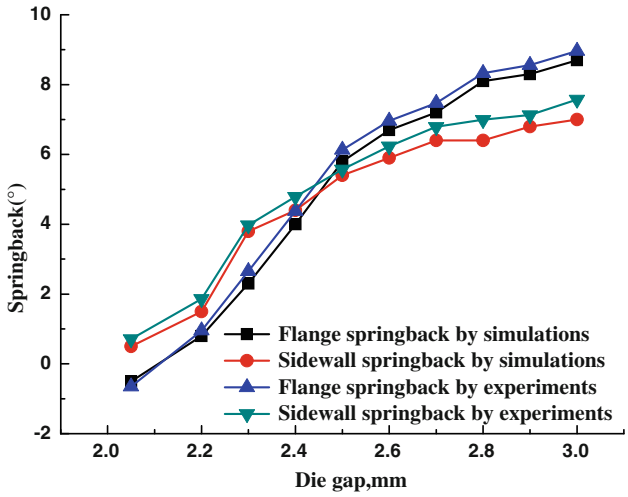

Fig. 13 Influence of die gap on the springback

increases, and both angles of θ_{sb} and θ_{sf} become more than 90°. During the hot forming process, the cooling of U-channel part is non-uniform, inner layer of blank remaining in contact with tools gets cooled at higher cooling rate than the outer layer in contact with air as shown in Fig. 14. Therefore, the inner layer shrinks sharply, the flange angle and sidewall angle are exerted by two flexural torques of M_1 and M_2 as shown in Fig. 14, and it leads to the decrease of θ_{sf} and θ_{sb}. Therefore, the springback becomes smaller, and the θ_{sf} becomes less than 90°, which is the cause of negative flange springback which is different from that in cold forming.

4.3 Influence of Forming Finishing Temperature on Springback and Mechanism of Springback in Hot Forming

Figure 15 shows the influence of forming finishing temperature (FFT) on springback, the results shown in Fig. 15 exhibit an apparent reduction in springback with FFT increasing, additionally, the amount of springback is decreased drastically at the FFT more than 716 °C. As shown in Fig. 15, the comparison between experiment results and simulation results shows that the FE numerical model for hot forming developed in this article are reliable. To examine the cause of the influence of the FFT on springback, the tensile loading-unloading tests are performed under isothermal conditions. The test consists of the following four stages: (a) heating specimen to a target temperature and holding for 10 min (load controlled), (b) loading to the displacement of 1.5 mm in 5 s (displacement controlled), (c) unloading to 0 kN in 5 s (load controlled), and (d) air cooling to room temperature (load controlled). The stress and strain are measured during loading and unloading. For the strain rate of 1.0 s^{-1} and different test temperatures, the strain-stress curves obtained in the test at deformation temperature of 600, 700, 800, and 900 °C are shown in Fig. 16 (Ref 14). As per the results shown in Fig. 16, creep strain occurs at elevated temperatures—the higher the test temperature is the larger the creep strain is. It is clear that the marked decrease of elastic

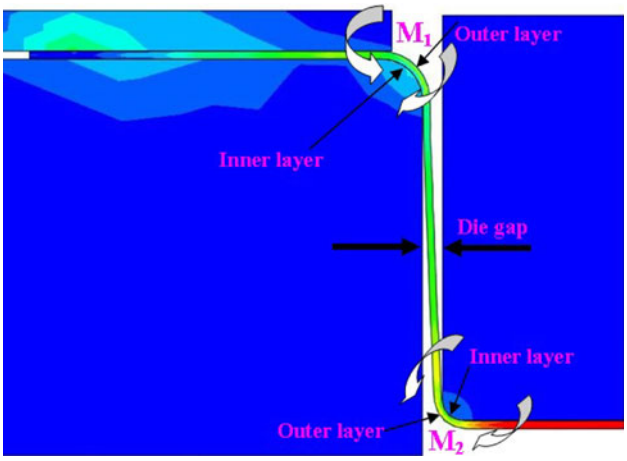

Fig. 14 Mechanism of springback

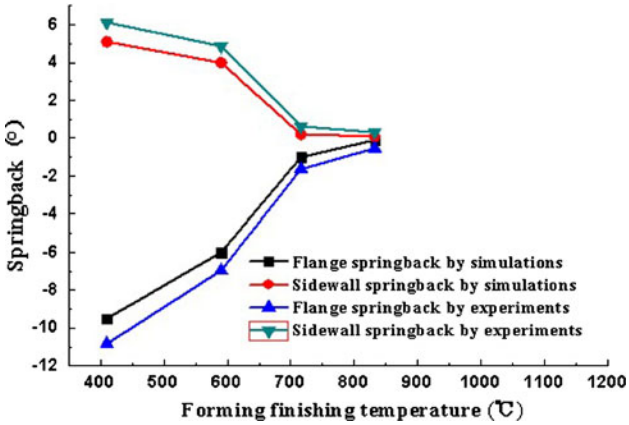

Fig. 15 Influence of forming finishing temperature on the springback

recovery is caused by the increase of high-temperature creep strain just after loading process. In general, it is said that tensile creep behavior and compressive creep behavior are different, but they are almost the same for such a short hot forming time. Therefore, the marked decrease of springback after hot forming can be explained through the increase of high-temperature creep strain in the releasing process. The strain recovery during unloading process reveals the mechanism of springback in sheet metal hot forming at elevated temperature.

5. Conclusions

(1) In order to exactly establish the FE model for hot forming process, the material's thermo-mechanical properties were investigated through tensile tests. It can be found that the strain, the strain rate, and the temperature have significant influence on the material flow stress. The reduction of material flow stress is more apparent—the higher the strain rate is the lower the temperature is. The constitutive model for describing the material's flow stress dependent on strain, strain rate, and temperature is developed.

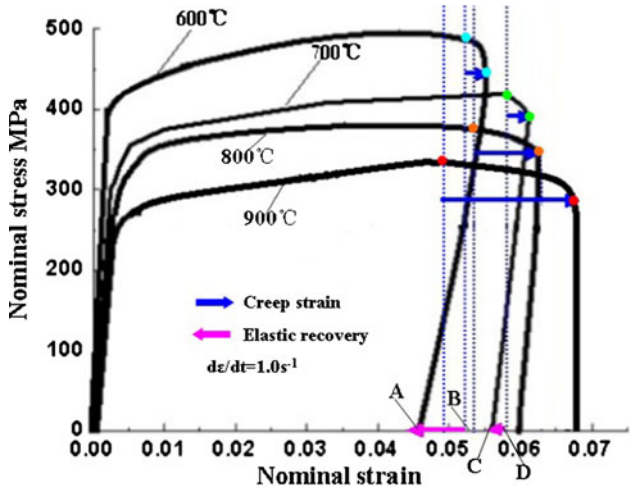

Fig. 16 Nominal stress-strain curve in the test at different test temperatures (Ref 14)

(2) Several important technologies associated with the numerical simulation of non-isothermal HSS sheet metal hot forming process, such as material modeling, treatment of contact including geometrical thermo-contacts meshing technologies, geometrical modeling, are solved successfully, based on the above technologies an exact FE model for hot forming is established.

(3) Numerical simulations of HSS sheet metal hot forming for U-channel part were carried out to investigate influence of two important processing parameters like BHF and die gap used in hot forming process. It can be concluded that BHF has a significant influence on the contact state between tools and blank as well as the distribution of temperature on flange, large BHF helps to reduce the amount of springback. Die gap has a considerable influence on the distribution of temperature on the sidewall of U-channel and thus the cooling rate of the sidewall during hot forming. The die gap is larger when the lower temperature on the sidewall is at the end of quenching stage. In addition, the processing parameters have a significant influence on the microstructure of U-channel part, and it reveals that the mechanical property of the hot-formed part depends on not only the material characteristics but also the processing parameters.

(4) The influence of hot forming finishing temperature on hot forming process is investigated. It is found that the forming finishing temperature has a significant influence on springback. Increasing forming finishing temperature increasing leads to an apparent reduction in springback. The mechanism of springback in non-isothermal hot forming was developed. The material creep behavior and the heat effect have played an important role in springback; the creep strain helps to reduce the springback, on the contrary, the heat effect leads to large amount of springback.

(5) The numerical results are in good consistency with experimental results. It also reveals that the FE numerical model developed in this article for hot forming is reliable in simulating the hot forming process.

Acknowledgments

This study was supported partly by China Postdoctoral Science Foundation under Grant 20080440846, the Heilongjiang Province Natural Sciences Foundation No. E2007-11 and the Project Supported by Development Program for Outstanding Young Teachers in Harbin Institute of Technology No. HITQNJS.2009.014.

References

1. M. Kleiner, M. Geiger, and A. Klaus, Manufacturing of Lightweight Components by Metal Forming, *Ann. CIRP*, 2003, **52**(2), p 521–542
2. J.X. Lu and L. Wang, Production and Usage of High Strength Sheet Metal Used in Automotive Industry, *Automob. Technol. Mater.*, 2004, **2**, p 1–6
3. P. Chen and M. Koc, Simulation of Springback Variation in Forming of Advanced High Strength Steels, *J. Mater. Process. Technol.*, 2007, **190**, p 189–198
4. T.B. Hilditch, J.G. Speer, and D.K. Matlock, Influence of Low-Strain Deformation Characteristics of High Strength Sheet Steel on Curl and Springback in Bend-Under-Tension Tests, *J. Mater. Process. Technol.*, 2007, **182**, p 84–94
5. G. Schiessl, T. Possehn, and T. Heller, Manufacturing A Roof Frame From Ultrahigh-Strength Steel Materials by Hot Stamping, *Proceedings, IDDRG*, Sindelfingen, 2004, p 158–166
6. R. Kolleck, D. Steinhoefer, J.A. Feindt, et al., Manufacturing Method for Safety and Structural Body Parts for Lightweight Body Design, *Proceedings, IDDRG, Sindelfingen,* 2004, p 167–173
7. K. Mori, S. Maki, and Y. Tanaka, Warm and Hot Stamping of Ultra High Tensile Strength Steel Sheets Using Resistance Heating, *CIRP Ann. Manuf. Technol.*, 2005, **54**, p 209–212
8. S.H. Choi and K.G. Chin, Prediction of Spring-Back Behavior in High Strength Low Carbon Steel Sheets, *J. Mater. Process. Technol.*, 2006, **171**, p p385–p392
9. J. Yanagimoto, K. Oyamada, and T. Nakagawa, Springback of High-Strength Steel after Hot, Warm Sheet Formings, *CIRP Ann. Manuf. Technol.*, 2005, **54**(1), p 213–216
10. M. Merklein, J. Lechler, and M. Geiger, Characterization of the Flow Properties of the Quenchenable Ultra High Strength Steel 22MnB5, *CIRP Ann. Manuf. Technol.*, 2006, **55**(1), p 229–232
11. M. Merklein, J. Lechler, and J. Mater, Investigation of the Thermo-Mechanical Properties of Hot Stamping Steels, *J. Mater. Process. Technol.*, 2006, **177**, p 452–455
12. B. Shapiro, Using LS-DYNA for Hot Stamping, *7th European LS-DYNA Conference*, 14–15 May 2009, Salzburg, Austria
13. M. Merklein and J. Lechler, *Determination of Material and Process Characteristics for Hot Stamping Process of Quenchable Ultra High Strength Steels with Respect to a FE-Based Process Design*, SAE Technical Paper Series, 2008-01-0853, SAE International, 2008
14. H. Liu, Z. Xing, J. Bao et al., Analysis of Mechanism of Springback in 22MnB5 High-Strength Steel Forming, *Acta Aeronautica et Astronautica Sinica*, 2010, **31**(4), p 865–870